**Climate
of the Past
Discussions**

Inorganic data from El'gygytgyn Lake sediments: stages 6–11

P. S. Minyuk[1], V. Ya. Borkhodoev[1], and V. Wennrich[2]

[1]North-East Interdisciplinary Scientific Research Institute of Far East Branch of Russian
Academy Science, Magadan, Russia
[2]University of Cologne, Institute for Geology and Mineralogy, Cologne, Germany

Correspondence to: P. S. Minyuk (minyuk@neisri.ru)

Discussion Paper | Discussion Paper | Discussion Paper | Discussion Paper

CPD

9, 393–433, 2013

Inorganic data from El'gygytgyn Lake sediments: stages 6–11

P. S. Minyuk et al.

Title Page

Abstract | Introduction

Conclusions | References

Tables | Figures

◀ | ▶

◀ | ▶

Back | Close

Full Screen / Esc

Printer-friendly Version

Interactive Discussion

Abstract

Geochemical study was performed on sediment of deep drilling core from El'gygytgyn Lake, located in central Chukotka, northeastern Russia (67°30′ N; 172°05′ E). Major and rare elements were determined by X-ray fluorescence spectroscopy (XRF) on 600 samples covering the timeframe between ca. 450 and 125 ka corresponding to Marine Isotope Stages (MIS) 11 to 6. Inorganic geochemistry data indicates significant variations in the elemental compositions corresponding to the glacials and interglacials periods. Interglacial sediments are characterized by high contents of SiO_2, Na_2O, CaO, K_2O, Sr and are depleted in Al_2O_3, Fe_2O_3, TiO_2, MgO. Extreme enrichments in SiO_2 during MIS 11.3 and 9.3 are caused by an enhanced flux of biogenic silica (BSi). Geochemical structure of stage 11 shows very similar peculiarities to features of stage 11 from records of Lake Baikal/SE Siberia and Antarctic ice cores. High contents of TiO_2, Fe_2O_3, MgO, Al_2O_3, LOI, Ni, Cr and Zr are typical for sediments of glacial stages, among those MIS 7.4 and 6.6 are the most marked. Peaks in the Fe_2O_3 content and coinciding low Fe_2O_3/MnO ratios during glacials indicate reducing condition in the sediments. This is also supported by enrichments in P_2O_5 and MnO, indicating an increased abundance of authigenic fine grained vivianite. Some elemental ratios indicate an enhanced alteration of glacial sediments accompanied by a loss of mobile elements, like Na, Ca, K and Sr. The higher alteration of sediments can presumably be traced back to changes in the sedimentation regime and diagenetic processes, and thus, reflects environmental changes.

1 Introduction

1.1 Location and setting

Lake El'gygytgyn is located in central Chukotka, northeastern Russia (67°30′ N; 172°05′ E). The lake measures approximately 12 km across and 174 m depth and is

placed in an 18-km wide meteorite crater (Fig. 1), which was created 3.58 ± 0.04 Ma in Upper Cretaceous volcanic rocks (Layer, 2000). Approximately 50 streams draining a catchments area of ca. 293 km^2 into the lake are mostly less than 5 km long (Nolan and Brigham-Grette, 2007). The Enmyvaam River as only outlet exits the lake to the south. The lake water is characterized low ion concentrations. Minimum and maximum values measured in spring and summer 2003 along vertical profiles through the water column at site Lz1024 and Lz1079 are: $Ca^{2+} = 0.71$–1.05 (Lz1024), 0.69–0.72 (Lz1079); $Mg^{2+} = 0.11$–0.19 (Lz1024), 0.11–0.12; $Na^+ = 0.53$–1.24 (Lz1024), 0.49–0.57 (Lz1079); $K^+ = 0.14$–0.19 (Lz1024), 0.18–0.22 (Lz1079). The pH values of 6.2–6.5 (Lz1024) and 5.7–5.9 (Lz1079) indicate that Lake El'gygytgyn is circumneutral to weakly acidic (Cremer and van de Vijver, 2006).

The catchments surrounding lacustrine basin to the north, west, and east primarily consists of ignimbrites and tuffs of the Pykarvaam and Ergyvaam Formations (Bely and Raikevich, 1994; Fig. 1b). The Voronian (ignimbrites, tuffs) and Koekvun' formations (andesite-basalts, tuffs, tuffaceous sands) are also present, but not as prevalent in the catchment area (Bely and Belaya, 1998; Bely and Raikevich, 1994). The crater rim is composed of hills reaching an altitude of 850–950 m.

According to geochemical data reported by Bely and Belaya (1998) the Pykarvaam and Ergyvaam formations are predominantly of acid composition and plot in the rhyolite field on total alkali-silica (TAS) diagram (Le Maitre et al., 2002; Fig. 2). Rocks of the Voronian formation are located in the andesite field, whereas Koekvun' formation plots in the basaltic andesite area. Chemical and physical weathering products from these rocks make up the majority of clastic deposition into the lake.

1.2 Inorganic geochemistry background

The first geochemical data of sediments from Lake El'gygytgyn were obtained from cores PG1351 (ca. 13 m) and Lz1024 (ca. 16 m) with basal ages of ~ 250 and 350 kyr BP, respectively (Minyuk et al., 2007, 2011). According to the distribution of major and rare elements, the core sequences were divided in geochemical zones

corresponding to MIS 1–10. It was shown that sediment from the warm climatic stages, which are represented by massive unstratified silts, are enriched in SiO_2, CaO, Na_2O, K_2O, and Sr, but are depleted and has low contents of TiO_2, Al_2O_3, MgO, Fe_2O_3, and LOI. Sediments from the cold stages are more chemically altered as visible in higher

5 values of the chemical index of alteration (CIA), plagioclase index of alterations (PIA), and the Rb/Sr ratio (Minyuk et al., 2007, 2011).

2 Methods

For elemental analyses, altogether 600 samples from the uppermost ca. 20 m of the composite profile of cores 5011-1 (Melles et al., 2011, 2012) were taken at regu-

10 lar 2-cm intervals. After freeze-drying, the samples were sieved to remove particles > 0.25 mm mostly consisting of rocks fragments and vivianite nodules. The major elements in the sediments were analyzed using a multichannel WDXRF spectrometers SRM-25 (USSR) and S4 Pioneer X-ray fluorescence spectrometer (Bruker, Germany). For analyses by the SRM-25 spectrometer, dry sediment samples were fused with

15 lithium tetraborate ($Li_2B_4O_7$) flux in a mass ratio of 1 : 1, and subsequently ground and layered with a boric acid base. X-ray fluorescence of $K\alpha$-lines was determined over a measurement time of 100 s by exposing the alloy to X-radiation generated by a Rh-anode tube set to 50 kV and 40 mA. Elemental compositions were determined using the fundamental parameters method (Borkhodoev, 2002). Wave-length dispersive X-

20 ray fluorescence analyses of elements were conducted by a Pioneer S4 spectrometer using a Rh-anode tube at voltage of 50 kV and a current 40 mA as primary radiation. The Pioneer S4 was equipped with a LiF200 analyzing crystal, a flow proportional detector, a collimator with angular aperture of 0.23° to register the analytical signal. The background near Ce $L\beta_1$ line was measured on the short wavelength side, while the

25 background near Ba $L\beta_1$ line was measured on long wavelength side.

Rare elements were determined by a VRA-30 XRF spectrometer (Germany). Sediment powders were measured in a cup with a 25 µm thick mylar window. The

intensity of the Rb, Sr, Y, Zr and Nb Kα-lines were determined after radiation with an Rh-anode at 50 kV and 40 mA. The elemental composition was achieved using the standard-background method. The Compton scattered Kα-lines of the X-ray tube target were used to correct for matrix effects and to determine the background radia-

5 tion (Borkhodoev, 1998). The lower detection limits of elemental determination by this method were 4 ppm for Rb, Y, Sr and Zr, and 3 ppm for Nb.

The loss on ignition (LOI) method was performed to estimate relative organic matter contents. Samples were heated to temperatures of 550 and 1000 °C over one hour, and the LOI was calculated from the weight loss was measured (Heiri et al., 2001).

10 Weight low-field AC magnetic susceptibility of discrete samples was measured on kappabridge MFK1-FA (AGICO Ltd., Brno, Czech Republic). Hysteresis parameters, including the saturation magnetization (J_s), induced magnetization (J_i), saturation remanence (J_{rs}), coercive force (B_c), and remanence coercivity (B_{cr}) were measured by an automatic coercive spectrometer (Burov et al., 1986). The relative content of the

15 paramagnetic component of magnetization (J_p) was calculated by the formula [J_i (at 500 mT) – J_s (ferromagnetic component)]/J_i (at 500 mT).

3   Results and discussion

The geochemical characteristics of lacustrine sediments depends on many factors including the chemical composition of provenance, physical and chemical weathering

20 processes in catchment, tectonic activity, sorting during sediment transport and sedimentation as well as diagenetic changes (e.g. Fralick and Kronberg, 1997).

3.1   Elemental concentrations

The various element distributions along the studied depth interval of the Lake El'gygytgyn core display significant parallel or opposite variations (Fig. 3). There are

25 strong negative correlation between SiO_2 and Al_2O_3 ($r = -0.89$), SiO_2 and Fe_2O_3

($r = -0.82$), SiO_2 and MgO ($r = -0.81$) and strong positive correlation between Al_2O_3 and Rb ($r = 0.82$), TiO_2 and MgO ($r = 0.83$), TiO_2 and Zr ($r = 0.82$), CaO and Sr ($r = 0.83$), K_2O and Rb ($r = 0.89$), K_2O and Ba ($r = 0.86$), Cr and Ni ($r = 0.78$) (Table 1). On the basis of the variability of the inorganic compounds, geochemical ratios, LOI, indices of chemical weathering and alterations the core sequence is divided into two groups of geochemical zones affected by different environmental conditions and climate occur during glacials/stadials and interglacials. Taking into consideration the age model based on magnetostratigraphy and tuning of proxy data to the regional insolation (Nowaczyk et al., 2007, 2013; Melles et al., 2012) the geochemical zones were correlated with marine isotope stages that are displayed on Fig. 3 as blue (cold stages) and yellow (warm stages) bars. Arabic numerals of the stages and substages on figures and in text are given in according to (Bassinot et al., 1994).

3.1.1 SiO_2

The SiO_2 content in the sediments of cold stages varies between 56.98 and 70.81 % (average 67.12 %), which is remarkably lower then SiO_2 content in the volcanic rocks of Pykarvaam and Ergyvaam formations (71.01 %). SiO_2 contents during warm stages averages 70.60 %. In two horizons at depths of 18.41–18.77 and 15.77–16.11 m the SiO_2 contents reach its maximum values in the entire sequence of 76.30 and 80.49 %, respectively. According to the age-depth model these horizons correlate to MIS 11.3 at 430–390 ka and MIS 9.3 at 340–320 ka. The SiO_2 enrichment in these zones is caused by high BSi contents and represents levels of high primary production in lake.

The Si/Ti ratio is positive correlated with biogenic silica and have been previously used as relative indicator of biogenic component in sediments of Lake El'gygytgyn (Melles et al., 2012) and Lake Baikal (Tanaka et al., 2007).

Large scale variations of the SiO_2 and TiO_2 contents indicate a generally strong negative correlation ($r = -0.74$) due to dilution of TiO_2 by biogenic silica. This strong correlation is especially valid for 70 samples from stages 11.3, 9.3 and partly 7.1 and 5.5 where SiO_2 exceed 71 %. The either very poor ($R^2 = 0.17$, interglacials) or lacking

linear correlation between SiO_2 and TiO_2 ($R^2 = 0.07$, glacials) for the remaining 530 samples from interglacials and glacial, respectively, suggest only a neglectable dilution by BSi (Fig. 4a). The strong positive correlation between SiO_2/TiO_2 and TiO_2/Al_2O_3 ($R^2 = 0.73$–0.75, Figs. 4b and 5) for these samples indicate that SiO_2/TiO_2 ratio related

5 to degree alteration of sediment.

SiO_2/Al_2O_3 ratios of interglacial and glacial sediments average 4.45 and 3.72, respectively, with constant SiO_2/Al_2O_3 ratios and a high linear correlation for warm stages ($R^2 = 0.88$), whereas sediments from cold stages are depleted in Al_2O_3 ($R^2 = 0.26$; Fig. 4d). A decrease in the SiO_2/Al_2O_3 ratio is considered to be either related to a de-

10 creasing grain size or a lower textural maturity (e.g. Weltje and Eynatten, 2004). Thus, the SiO_2/Al_2O_3 data of Lake El'gygytgyn indicate sediments from cold stages to consist either of more fine-grained material or to be more matured. The first is supported by grain-size data showing higher clay to fine silt contents during glacial times (Francke et al., 2013). In contrast, higher mean SiO_2/Al_2O_3 ratio of bedrock samples from the

15 Pykarvaam and Ergyvaam Formations of 4.70 indicate the lower maturity of the fresh rocks compare to the lake sediments.

3.1.2 TiO_2, Al_2O_3, Fe_2O_3

In lacustrine environments, the contents of Ti and Al have previously shown to be good measures of intensity of detrital input (Whitlock et al., 2008), rainfall intensity and

20 runoff (Juyal et al., 2009), as well as the flooding season (Yi et al., 2006) and catchment erosion (Panizzo et al., 2008).

The concentrations of TiO_2 and Al_2O_3 are enriched in the glacial sediments, with mean Al_2O_3 contents of 16.36 and 18.08 % and mean TiO_2 contents of 0.61 and 0.82 % during interglacials and glacials, respectively. The mean TiO_2 and Al_2O_3 contents of

25 rocks of the Pykarvaam + Ergyvaam formations are 0.36 and 15.15 %, respectively.

The good correlation of Al_2O_3 and SiO_2 (Fig. 4c) indicate the overall Al_2O_3 variations on a interglacial/glacial scale to be largely triggered by variations in the BSi flux. The

weak correlation of SiO_2 and TiO_2 imply a only minor dilution effect, which is restricted to peak interglacials. In contrast, Ti seams to be more controlled by grain-size variations. Sediments of warm stages consist of massive silt, while the cold stage sediments comprise of laminated silt and clay (Francke et al., 2012; Melles et al., 2011, 2012).

Thus, titanium is supposed to be mainly concentrated in the fine fraction. This is also supported by the lower TiO_2 concentrations in the bedrock samples. A similar enrichment of Ti in the silt and clay fraction is also documented for weathered granitic rocks in Spain (Taboada et al., 2006) or Archaean rock in Canada (Fralick and Kronberg, 1993).

The TiO_2/Al_2O_3 ratio that has been often used as an indicator of the provenance of sediments but also on the degree of sediment alteration (Migdisov, 1960; Young and Nesbitt, 1998; Yudovich and Ketris, 2011) averages 0.037 and 0.045 in warm stage sediments and cold stage sediments, respectively, and 0.032 in the unweathered volcanic rocks. The Al_2O_3 vs. TiO_2 diagram show a rather straight, linear trend for interglacial sediments ($R^2 = 0.55$), while cold sediments display scatter distribution ($R^2 = 0.024$) (Fig. 4e). Higher TiO_2/Al_2O_3 ratios during glacial periods in combination with lower Al_2O_3 contents suggest a higher alteration intensity, likely due to the loss of Al-rich phases under intense weathering (Young and Nesbitt, 1998). On the other hand, higher titanium contents in finer-grained cold stage sediments also cause the TiO_2/Al_2O_3 ratios to raise.

Mean Fe_2O_3/Al_2O_3 ratio averages 0.30 and 0.35 in interglacials and glacials, respectively, but is diminished in the surrounding volcanic rocks (0.28). The Fe_2O_3–Al_2O_3 diagram exhibit a linear correlation during warm stages ($R^2 = 0.33$), whereas glacial sediments display large scatter ($R^2 = 0.001$) (Fig. 4f). As visible in the parallel trend of TiO_2 and Fe_2O_3, SiO_2/TiO_2 and SiO_2/Fe_2O_3 and the positive correlation in the TiO_2–Fe_2O_3 diagram ($R^2 = 0.48$) (Figs. 3, 4d and 5), iron behaves very similar to titanium.

To investigate the Fe and Ti mineralogy in Lake El'gygytgyn sediment, we investigated the correspondence of both elements to various magnetic parameters. During glacial periods, sediments exhibit high Fe_2O_3 and TiO_2 contents but low a magnetic

susceptibility (MS), whereas interglacial sediments display the opposite. Consequently, data on Fe_2O_3–MS and TiO_2–MS diagrams show a scatter distribution (Fig. 6a and b) with low negative correlation coefficients (r) of -0.28 and -0.43 for Fe_2O_3 vs. MS, and TiO_2 vs. MS, respectively. This contradicts an enrichment of Ti and Fe in the detrital

5 heavy mineral fraction, which has shown to be mirrored by a generally positive correlation of TiO_2 and Fe_2O_3 to the MS (e.g. Ortega et al., 2006; Parker et al., 2006; Reynolds et al., 2006; Vegas et al., 2010). MS includes both ferromagnetic and paramagnetic components that can be distinguished by determining the induced magnetization. TiO_2 and Fe_2O_3 yield only a very poor correlation to the ferromagnetic component

10 (J_f) (Fig. 6c and d), but a strong correlation to the paramagnetic component (J_p) of induced magnetization (Fig. 6e and f). Hence, high TiO_2 contents in the glacial sediments don't attribute to the typical ferromagnetic titaniferous minerals in sediments, like rutile, ilmenite or titanomagnetite, which would evoke a positive correlation of TiO_2 (Fe_2O_3) to MS and J_f. Thus, most Ti and Fe especially in the sediment of cold stages

15 is supposed to be concentrated in paramagnetic Fe- or Ti-bearing minerals, like chlorite ($Mg_{3.5}Fe_{1.5}Al_2Si_3O_{14}$) with Fe and Mg acting as main elements (Boyle, 2002). The importance of chlorite as one main iron carrier in glacial sediments is indicated by a positive correlation of TiO_2 to MgO ($r = 0.83$) and Fe_2O_3 to MgO ($r = 0.65$). This is supported by clay mineral analyses of Lake El'gygytgyn sediments of the past 65 ka

20 showing cold stages to be typically enriched in chlorite (Asikainen et al., 2007).

3.1.3 P_2O_5, MnO

P_2O_5 and MnO concentrations show a parallel with strong fluctuations throughout the core profile (Fig. 3) resulting in a correlation coefficient of 0.55. Both elements are strong positively correlated to Fe_2O_3 (Table 1). Peak contents of P_2O_5 and MnO were

25 found at depth of 18.85–18.39, 13.51–13.19, 12.19–11.51, 9.21–8.71, 7.26–6.99, and 6.65–6.39 m. Most of these intervals are attributed to the early parts of cold stages, as MIS 8.4, 7.4, 6.6, 6.4, and 6.2 with exception of the lowest interval (18.85–18.39 m) that corresponds to super interglacial MIS 11.3. All of these intervals exhibit high LOI

values as a proxy for relative content of organic matter (Fig. 5). These parallel enrichments in MnO and P_2O_5 and Fe_2O_3 are linked to the occurrence of authigenic fine-grained vivianite, whose formation is primarily controlled by Fe and P supersaturated porewaters, anoxic condition as well as the appearance of organic matter (Sapota

⁵ et al., 2006). Electron-microprobe analyses reveal the presence of Fe_2O_3, P_2O_5 and MnO in nodules of vivianite. The Fe_2O_3 content in these nodules varies from 30.18 to 39.4 % (35.18 % in average), while P_2O_5 and MnO concentrations varies from 21.23 to 29.28 % (25.02 % in average), and from 0.67 to 6.34 % (2.06 % in average), respectively (Minyuk et al., 2012). Mn is described as a typical impurity in Baikal Lake vivianite

¹⁰ (Fagel et al., 2005). In few samples from MIS 6 Fe-Mn aggregates could be identified by energy dispersive spectroscopy. Fe and Mn reacts very sensitive but slightly different to changes in the oxic-anoxic conditions, and thus, the Mn/Fe (or Fe/Mn) ratio is commonly used as indicator for palaeo-redox environments (e.g. Davison, 1993; Loizeau et al., 2001; Melles et al., 2012). Low values of the MnO/Fe_2O_3 ratio dominate

¹⁵ in glacial sediments suggesting anoxic conditions in the bottom water and surface sediment during sedimentation (Figs. 4g, 5). Plots of Fe_2O_3 and the MnO/Fe_2O_3 ratio show a parallel behavior for the early intervals of MIS 6.6 and 7.4 and some levels during MIS 11.3. These are characterized by maxima of the Fe_2O_3 content and maxima of the MnO/Fe_2O_3 ratio accompanied by the occurrence of fine-grained vivianite indicating

²⁰ reducing condition in the lake (Mackereth, 1966).

3.1.4   Cr, Ni

The concentrations of Cr and Ni in the sediments of Lake El'gygytgyn fluctuate between 8 and 333 ppm (65 in average), and 9 and 1032 ppm (49 in average), respectively. Both elements exhibit a very similar down-core distribution (Fig. 3) as also indicated

²⁵ by a strong positive correlation ($r = 0.78$) (Fig. 4h, Table 1). Chromium and nickel are generally enriched during cold stages and MIS 11.3 but are depleted in warm stages (Fig. 3). The first are characterized by high abundances of total organic carbon (Melles et al., 2007, 2012), LOI (Fig. 5), and higher clay contents suggesting that Cr and Ni

might be absorbed by organic matter (e.g. Sharma et al., 2004) or clay minerals (e.g. Das and Haake, 2004; Pistolato et al., 2006). Geochemistry of surface sediment of lake indicates that main source of Cr and Ni are basaltic weathering product of southern shore (Wennrich et al., 2012).

3.1.5 Zr, Rb, Sr, Ba

Zr, Rb and Sr contents vary in the investigated sediment sequence of Lake El'gygytgyn between 81 and 257 ppm (172 ppm in average), 52 and 154 ppm (105 ppm in average), 112 and 249 ppm (187 ppm in average), respectively. The Sr content in the dominating Pykarvaam and Ergyvaam Formations averages 285 ppm. Rubidium shows a high positive correlation to Al_2O_3 ($r = 0.82$) and to K_2O ($r = 0.89$). Rubidium is in general negatively correlated to zirconium ($r = -0.66$), except for sediments of super interglacial stages 9.3 and 11.3 when both elements exhibit a parallel distribution presumably due to dilution by highest BSi contents. Zr shows strong positive correlation with TiO_2 ($r = 0.82$) and Sr is positive correlated with CaO ($r = 0.83$) (Table 1).

The Rb/Sr ratios of interglacials and glacials varies from 0.32 to 1.03 (mean 0.52, $n = 308$) and between 0.41 and 1.24 (mean 0.62, $n = 292$), respectively. This is significantly higher then the average Rb/Sr ratio of volcanic rock surrounding Lake El'gygytgyn of 0.32 ($n = 18$) being very close to those from Upper Continental Crust (0.32) (Taylor and McLennan, 1985). As strontium as a mobile element gets lost during chemical weathering the rocks, thus, the resulting Rb/Sr ratio in weathered rock increases relative to fresh (e.g. Dasch, 1969). Hence, the Rb/Sr ratio have been applied to define provenances and elucidate the weathering history of different type of deposits including deep-sea, alluvial, lacustrine sediments, loess and paleosoils (e.g. Gallet et al., 1998; Goldberg et al., 2000). The increased Rb/Sr ratios of glacial sediments of Lake El'gygytgyn with respect to warm stages and surrounding rocks indicates a systematic Sr depletion due to higher alteration and seams to be controlled by grain-size variations as was report for Teletskoe Lake (Kalugin et al., 2007).

|◀ | ▶|

◀ | ▶

Back | Close

Full Screen / Esc

Printer-friendly Version

Interactive Discussion

The Rb/Sr ratio strong positively correlated with Ba/Sr ratio (Table 2) used as an indicator of weathering and leaching intensity of sediments (e.g. Goldberg et al., 2000; Yang et al., 2006; Bokhorst et al., 2009). The Ba/Sr ratios vary from 1.60 to 4.10 (2.41 in average, $n = 302$) in interglacial and between 2.15 and 4.49 (2.72 in average, $n = 292$) in glacial sediments. The Ba and Rb content are strong positive correlated with K_2O (Table 1) support a K-feldspar source for these elements.

3.2 Geochemical indices

Different geochemical indices are used for quantitative estimations of alteration and weathering of rocks (e.g. Duzgoren-Aydin et al., 2002; Maslov et al., 2003; Price and Velbel, 2003; Yudovich and Ketris, 2011). Most of the indices are expressed as molecular or weight percentages of various oxides or groups of oxides. During chemical weathering, more labile minerals, like feldspar, are depleted in Ca^{2+}, K^+ and Na^+ and transform to minerals that are more stable under surface conditions. As the intensity of weathering increases, Al, Ti, Fe, and Mn become enriched in weathered rocks and sediments.

The distribution of selected indices exhibits parallel or opposite variations along the investigated sediment sequence (Fig. 5), with several indices being evaluated in Lake El'gygytgyn sediments (Table 2).

3.2.1 Chemical index of alteration

Chemical index of alteration (CIA) was defined by Nesbitt and Young (1982) using molecular proportions:

$$CIA = [Al_2O_3/(Al_2O_3 + CaO + NaO + K_2O)] \cdot 100, \tag{1}$$

with CaO being the amount of CaO incorporated in the silicate fraction of the rock. CIA measures the proportion of Al_2O_3 versus more labile oxides and reflects the proportion of feldspars and clay minerals. According to Nesbitt and Young (1982), CIA for

unaltered albite, anorthite and potassic feldspar averages 50, and measures 30–40 for basalt, 45–55 for granites and granodiorites, 75–85 for illite, 75 for muscovite, and close to 100 for kaolinite and chlorite.

The CIA index has been previously used for estimations of the climatic control on chemical changes in various environments of different ages, including lacustrine sediments (e.g. Roman-Ross et al., 2002; Das and Haake, 2003; Roy et al., 2010). However, the CIA not exclusively reflects climatic conditions during weathering in the catchment, but can be influenced by post-deposition modifications of clay minerals, such as diagenetic illitization of smectite, which complicates estimation of alteration (Xiao et al., 2010).

In the sediment sequence of Lake El'gygytgyn, the CIA varies between 59.91 and 76.16 (65.84 in average) during warm and between 62.69 and 75.15 (69.40 in average) during cold stages (Fig. 5). Volcanic rocks of the El'gygytgyn area, in contrast, exhibit a CIA of 43.70–56.32 (49.71 in average).

Silicate weathering trends can be inferred from the Al_2O_3–$(CaO + Na_2O)$–K_2O ternary diagram (Nesbitt and Yang, 1984). For the sediments of Lake El'gygytgyn an obvious trend line parallel to the Al_2O_3–$(CaO + Na_2O)$ boundary indicates a progressive depletions of Ca and Na during weathering in preference to K. Volcanic rocks plots close to the plagioclase-K-feldspar join line (Fig. 7a) supposing that feldspars are the dominant Al-bearing minerals. Beach pebbles from the lake, in contrast, plot slightly above the plagioclase-K-feldspar join line indicating a rather low chemical weathering. Sediments from cold and warm stages show an intermediate intensity of alteration with higher value for cold sediment (Fig. 7a). In general, sediment data plots below the smectite-illite join line suggesting that sediments of warm stages contain more feldspar. Enhanced concentrations of feldspar of surface sediment of Lake El'gygytgyn are linked to the high content of sand (Wennrich et al., 2012).

3.2.2 Plagioclase index of alteration

The plagioclase index of alteration (PIA) enables to estimate the weathering intensity of plagioclase (Fedo et al., 1995) and is calculated according to the following equation:

$$[(Al_2O_3 - K_2O)/(Al_2O_3 + CaO + Na_2O - K_2O)] \cdot 100. \tag{2}$$

The PIA in the Lake El'gygytgyn record vary from 63.81 to 86.35 (mean 71.80) in interglacial and from 67.44 to 84.92 (mean 75.95) in glacial sediments. Volcanic rocks of the lake catchment exhibit much lower PIA values of 43.02–59.79 (mean 49.99). The PIA of the pelagic sediments shows a strong positive correlation to other weathering indices (Table 2).

As demonstrate in the ternary diagram $CaO–(Al_2O_3-K_2O)–Na_2O$ (Fig. 7b), sediment data and values of the dominating Pykarvaam and Ergyvaam Formations are located in the central part of diagram with a slight shift to the albite composition. The position of the glacial sediments closer to the $Al_2O_3-K_2O$ apex of the diagram suggests a higher alteration compared to interglacial deposits (Fig. 7b).

3.2.3 Chemical index of weathering

The chemical index of weathering (CIW) was proposed by Harnois (1988) and is calculated using the equation:

$$CIW = [Al_2O_3/(Al_2O_3 + CaO + NaO)] \cdot 100, \tag{3}$$

with Al_2O_3 treated as an immobile component, and CaO and Na_2O used as mobile elements. Potassium, in contrast, is not involved because it may be leached or accumulated in the residual weathering products. Fedo et al. (1995) point out that aluminum in this index is used without any correction for Al in K-feldspar, and therefore K-feldspar–rich rocks yield very high CIW values. Potassic granite, for example, has a CIW of 80 and fresh K-feldspar has a CIW of 100, which is similar to values for residual products

Title Page

Abstract | Introduction

Conclusions | References

Tables | Figures

|◄ | ►|

◄ | ►

Back | Close

Full Screen / Esc

Printer-friendly Version

Interactive Discussion

of chemical weathering (smectite: 80; kaolinite, illite, and gibbsite: 100) (Fedo et al., 1995).

The CIW ranges from 69.03 to 88.58 (72.28 in average) during interglacials and increase to 72.39–87.43 (79.42 in average) during glacial periods due to the depletion of Na and Ca relative to Al. In unweathered volcanic rocks of El'gygytgyn area index vary from 45.94 to 68.47 (mean 56.17).

3.2.4 Chemical proxy of alteration

The chemical proxy of alteration (CPA) (Buggle et al., 2010) is defined as:

$$Al_2O_3/(Al_2O_3 + Na_2O) \cdot 100. \tag{4}$$

The CPA does not involve silicate CaO that difficult estimate in calcareous sediments and potassium because of its inconsistent behavior during chemical weathering. Index was proposed as geochemical proxy of silicate weathering for loess and paleosoil.

The CPA index of volcanic rock of El'gygytgyn area varies from 62.16 to 79.80 (average 73.33). In the sediments of Lake El'gygytgyn, the CPA value in sediments of warm stages ranges from 77.13 to 93.27 (average 82.82), whereas glacial sediments show CPA value between 80.70 and 92.18 (average 85.17) indicating high intensity of alteration of glacial sediment. The index is strong positively correlated with CIA, CIW and PIA in spite of K_2O and CaO does not involve for calculation (Table 2).

3.2.5 $(CaO + Na_2O + MgO)/TiO_2$ index

The ratio was defined for decarbonated sediments and is used to estimate the weathering intensity of loess deposits (Yang et al., 2006). In contrast to the previous element ratios, titanium is used as immobile component in this ratio. Yang et al. (2006) point out that the $(CaO + Na_2O + MgO)/TiO_2$ ratio behaves independently of grain size effects, and thus, the influence of transport-driven mineral differentiation is eliminated to a large extent.

In Lake El'gygytgyn sediments the ratio varies from 6.45 to 13.58 with interglacials showing a ratio of 7.39 to 13.58 (mean 10.2, $n = 308$) and glacials exhibiting ratios between 6.45 and 11.26 (mean 8.13, $n = 292$). The values of this index show parallel but reverse fluctuations to other indices, except for MIS 6.6 and 7.4 where lowest values correspond to high TiO_2 contents (Fig. 5). Volcanic rocks indicates index value of 17.8–42.2 (average 26.9, $n = 19$).

3.2.6 Silica–Titania index

The Silica–Titania index (STI) (de Jayawardena and Izawa, 1994) is defined as:

$$[(SiO_2/TiO_2)/((SiO_2/TiO_2) + (SiO_2/Al_2O_3) + (Al_2O_3/TiO_2))] \cdot 100, \tag{5}$$

and was developed to estimate the degree of chemical weathering of metamorphic silicate rocks.

The STI averages 84.39 and 82.17 for interglacial and glacial sediments, respectively, and 84.35 for volcanic rocks of El'gygytgyn area. In El'gygytgyn SiO_2 can be both of detrital and biogenic origin, and thus, the index rather reflects the relative intensity of primary diatom production than a geochemical alteration of sediments.

3.3 Geochemical indices as proxy for environmental changes

The distribution of geochemical varies between glacial and interglacial sediments suggesting different environmental condition. Glacial intervals show high values of CIA, CIW, PIA, CPA, Rb/Sr, Ba/Sr, LOI and low values of STI and the $(CaO + Na_2O + MgO)/TiO_2$ ratio. The glacial sediments are higher altered compared to interglacial and volcanic rocks and depleted by potassium, sodium, calcium and strontium. This feature can be used for discrimination of the glacial and interglacial sediments. One possible explanation for the marked difference is that glacial sediments were more chemically weathered than interglacial sediments. It is considered that chemical weathering increase in warm and wet climate, although chemical weathering

is also active under cold climatic conditions (e.g. Darmody et al., 2000; Hall et al., 2002). Nevertheless, temperature and precipitation have been shown to be the main drivers of chemical weathering rates in watersheds (e.g. White and Blum, 1995). Surprisingly sediments from the super interglacial MIS 11.3 exhibit rather low weathering

5 indices compared to glacial sediments, although maximum summer temperature and annual precipitation values of ~ 4 to $5\,°C$ and $\sim 300\,mm$, respectively, higher than those of Holocene were reconstructed (Melles et al., 2012). Hence, climate-driven changes of the chemical weathering regime in the lake catchment on a glacial and interglacial timescale as origin of the geochemical difference of sediments are rather unlikely.

10 Furthermore, glacial to interglacial variations in the sediment geochemistry could be caused by changes in the provenance. But this explanation can be excluded due to the nature of Lake El'gygytgyn as a closed basin with a very restricted watershed bordered by the crater rim. Alternatively, the highly weathered material could have been transported by eolian processes from remote regions. Comparison the geochemical similar-

15 ity of dominating volcanic rocks, pebbles and lake sediments disprove this suggestion. On the ternary Al_2O_3–$(CaO + Na_2O)$–K_2O and CaO–$(Al_2O_3$-$K_2O)$–Na_2O diagrams the various El'gygytgyn data plot parallel to the $(CaO + Na_2O)$–Al_2O_3 and Na_2O–$(Al_2O_3$-$K_2O)$ axes, respectively, clearly indicating local volcanic rocks to be the major source of clastic material at the lake floor. Thus, any eolian input into the lake during glacials

20 must derive from local weathering products of these rocks.

It is considered that grain-size sorting and diagenetic processes are important factors influencing the dissimilarity of geochemical indices. In Lake El'gygytgyn sediments three main lithological facies were defined indicating different sedimentation and transport conditions during glacials and interglacials (Melles et al., 2012). Glacial sediments

25 (Facies A) consist of dark gray to black laminated silt and clay, whereas interglacial deposits (Facies B) are composed of olive-gray to brownish massive to faintly banded silt. Sediments of super interglacials (Facies C), such as MIS 11.3, in contrast, consist of reddish-brown finely laminated silt (Melles et al., 2012). Asikainen et al. (2007) pointed out that chlorite is the typical clay mineral in glacial sediments, whereas smectite

and illite are more abundant during interglacials. This is consistent with the distribution of major elements in sediment. Grain-size data of the clastic fraction (without organics, biogenic silica and vivianite crystals) indicate that sediment of MIS 1 contains more silty than glacial sediments richer in clay (Asikainen et al., 2007). According to Francke et al. (2013) warm periods are characterized by coarser hemipelagic sediments whereas finer ones occur during cold periods. A perennial ice cover on lake during peak glacial intervals obviously restricted the transport of coarse-grained less weathered sediments but enabled finer particles to be transported to central part of lake basin through cracks or moats around the shore in during summer (Asikainen et al., 2007). On other hand, precipitation was increased during interglacials, which together with geomorphology of crater slopes tends to favor erosion and denudation of weathered material to the lake. Permafrost in the lake vicinity promoted cryogenic weathering and solifluction processed with higher rates on south-facing slopes (Schwamborn et al., 2008).

Furthermore, the geochemical data imply that the sediment composition is additionally modified by in-lake processes complicating the interpretation of geochemical indices.

Interglacial sediments of MIS 9.3 and 11.3 and partly of MIS 7.1 and 5.5 show significantly higher BSi contents (Melles et al., 2012; Fig. 3) leading to a dilution of terrigenous material.

On the other hand, diagenetic processes obscured the detrital geochemical signals. The glacial facies is supposed to be accumulated under anoxic bottom water conditions (Melles et al., 2007, 2012) resulting in a dissolution of magnetic minerals (Nowaczyk et al., 2007). The formation of authigenic vivianite, Fe-Mn aggregates, pyrite and greigite indicates a strong post-depositional alteration of sediments during anoxia, which can also lead to partial dissolution of silicates are also accompanied by a loss of cations (Wallmann et al., 2008). A similar cations depletion in anoxic glacial sediments might explain high CIA, CIW, PIA, CPA values.

Obtained data indicate that geochemical indices and selected elemental ratios mirror sedimentation conditions and diagenetic processes that are triggered by environmental and climate changes during glacials and interglacials.

4   Geochemical structure of MIS 11

Marine isotope stage 11 is known to be the warmest and longest interglacial interval of the past 500 ka (e.g. Howard, 1997), and can be subdivided in substages 11.1, 11.22, 11.23, 11.24 and 11.3 (Bassinot et al., 1994).

On the basis of geochemical data substage 11.3 is further divided into three zones (Fig. 8). The lower zone (a) is characterized by a gradual increase of SiO_2, Na_2O, K_2O, CaO, Sr, and STI, and a decrease of TiO_2, Al_2O_3, MgO, Fe_2O_3, LOI, CIA, CIW, PIA, CPA typical for all warm stages. At 5 levels visible vivianite nodules (> 0.25 mm) were found, and at additional 10 levels sediment includes coarse grains of sand and gravel that are supposed to be formed by ice-rafting during the break-off of the lake ice cover. Zone a is characterized by a distinct peak of geochemical data that resembles the distribution of biogenic silica in Lake Baikal (Prokopenko et al., 2006, 2010) and temperature reconstructions derived from the Antarctic ice core records marked as event 11.33 (Spahni et al., 2005).

The middle zone (b) of substage 11.3 exhibits a sharp SiO_2 increase due to a pronounced BSi maximum (Melles et al., 2012). A simultaneous drop to minimum values of TiO_2, Al_2O_3, MgO, but also Na_2O, CaO, K_2O, Rb, Sr, Zr, and Ba can presumably be traced back to dilution by biogenic silica. On the other hand, values of LOI, Cr and Ni are remarkably increased during zone b as common for glacial intervals, but the Ni and Cr peaks do not coincide with those of other elements. Sharp parallel variations of the P_2O_5, MnO, Fe_2O_3 contents in this zone are displayed by P_2O_5/MnO, Fe_2O_3/MnO, and Fe_2O_3/P_2O_5 correlation coefficients of 0.93, 0.86 and 0.94, respectively. These elements are supposed to be contained in fine grained vivianite as proven smear-slides. In contrast to glacial sediments, vivianite nodules > 0.25 mm don't occur in this interval.

The very high SiO_2 contents exhibit a saw-toothed distribution and behave in antiphase to the P_2O_5, MnO and Fe_2O_3 contents (Fig. 8) as obvious in the high negative correlation coefficient between SiO_2 and Fe_2O_3 of −0.50. Furthermore, numerous peaks of Fe_2O_3 and corresponding maximum of MnO/Fe_2O_3 ratio indicating reducing conditions
5   on these levels. This suggests that the apparent lamination of the MIS 11.3 sediments builds up of alternating layers of highly biogenic sediments enriched in SiO_2 deposited under oxic conditions at the bottom lake and sediments less enriched in SiO_2 but with abundant Fe, P and Mn that is supposed to be formed under anoxia. Even in the oxic horizons, MS exhibits only low values presumably due to the dilution of magnetic min-
10 erals by BSi. But in contrast to low MS minima in anoxic glacial sediments, the low paramagnetic component of magnetization suggests an only negligible dissolution of magnetic minerals. Absent coarse-grained components in zone b, like sand and gravel, imply only minor active ice-rafting. The alternation of oxic and anoxic horizons indicates that anoxic condition at the water-sediment interface caused by decomposition
15 of organic matter on bottom lake were promoted by an enhanced bioproduction under favorable highly oxygenated conditions in middle and upper parts of water column.

Upper zone (c) of substage 11.3 is characterized by a gradual decrease of SiO_2, LOI, Ni, Cr and a simultaneous increase of TiO_2, MgO, Fe_2O_3, Al_2O_3 and other elements as well as the absence of P_2O_5 and MnO peaks, vivianite nodules and coarse sediments.
20 In substages MIS 11.2–11.1 (depth 18.07–17.11 m) the SiO_2 content ranges between 66.92–69.97 % (68.65 in average) and exhibits only minor variations. The TiO_2 content displays four distinct minima at a depth of 17.87, 17.73, 17.61 and 17.29 m corresponding to peak values of CIA, STI, PIA, CIW, and CPA. There is very poor negative correlation between TiO_2 and Fe_2O_3 ($r = -0.15$). The common occurrence of
25 coarse sand and gravel in the substage 11.2 might indicate enhanced ice rafting. The absences of vivianite nodules in substage 11.1 imply well oxygenated bottom water conditions.

Geochemical structure of MIS 6.6 and 7.4

Among the glacials substages, MIS 7.4 and 6.6 are most pronounced and show similar geochemical features. As visible in the element distribution of MIS 7.4 (Fig. 9), these full glacial sediments are characterized by lowest contents of SiO_2 suggesting a low
5 or absent biogenic sedimentation. Synchronously, TiO_2, Fe_2O_3, MgO, Al_2O_3 and Zr are extremely enriched. There are few specific similarities in the geochemical behavior of stage 7.4, 6.6 and other glacials. Almost all geochemical characteristics including elements, indices and ratios start to react to the climate change simultaneously. The contents of TiO_2 increase gradually to maximum.
10 The lower parts of these substages marked as zone a (Fig. 9) are characterized by a sharp decrease of the SiO_2 content suggesting a diminished biogenic accumulation. High peaks of Fe_2O_3, P_2O_5, MnO, Mn/Fe_2O_3, and LOI are indicating reducing condition in the bottom water and at the sediment/water interface accompanied by the precipitation of Fe-bearing minerals, like vivianite and/or Fe-Mn aggregates. The lack
15 of large vivianite nodules in these intervals suggests a direct precipitation fine grained vivianite from the lake water presumably triggered by a climatic and/or environmental deterioration. Low magnetic susceptibility and high J_p values suggest the dissolution of magnetic minerals. In contrast, the absent correlation between J_p and the phosphorus and manganese contents suggests phyllosilicates as probable main paramagnetic
20 minerals in sediments. Abundant coarse sand points to an intensified ice-rafting.
The middle part of substage 7.4 (zone b) and the lower part of substage 6.6 are enriched in Ni and Cr and show high value of LOI. Concentrations of K_2O, CaO, Na_2O, Sr, Rb, Ba are low but higher than during MIS 11. The sediment of zone b don't contain any coarse material suggesting a permanent ice cover with only narrow moats in
25 summer seasons that restricted ice moving, and thus, a transport of coarse-grained material into the lake center.
In zone (c) again abundant coarse material occur. Geochemically, the sediments of zone (c) take an intermediate state between those glacials and interglacials.

5   Conclusions

The inorganic geochemistry of Lake El'gygytgyn sediments indicates distinct downcore variations of the elemental compositions over the past ca. 500 ka corresponding to the glacial and interglacial periods. Interglacial sediments show high contents of SiO_2, Na_2O, CaO, K_2O, and Sr but the low contents of Al_2O_3, Fe_2O_3, TiO_2, and MgO. Glacial sediments, in contrast, exhibit opposite distribution. Peaks in P_2O_5 and MnO coincide with an increased abundance of fine grained vivianite indicating temporal reducing conditions in the sediment and/or bottom waters. Super interglacial stages 9.3 and 11.3 are enriched in SiO_2 due to the increased flux of biogenic silica tracing a maximum diatom production. The geochemical structure of MIS 11 shows very similar peculiarities to features of this isotope stage in records from Lake Baikal and Antarctica. Among the glacials substages, MIS 7.4 and 6.6 are the most marked and are characterized by lowest contents of SiO_2 suggesting low or absent of primary production by diatom and very high contents of TiO_2, Fe_2O_3, MgO, Al_2O_3 and Zr. Peaks of the Fe_2O_3 content coincide with high MnO/Fe_2O_3 ratios indicating reducing condition in the sediments and/or bottom water.

Geochemical indices and some elemental ratios indicate a higher alteration of glacial sediments accompanied by a depletion of mobile elements, such as Na, Ca, K and Sr. This alteration might be caused by the sedimentation regime and/or post-depositional diagenetic processes.

References

Asikainen, C. A., Francus, P., and Brigham-Grette, J.: Sedimentology, clay mineralogy and grain-size as indicators of 65 ka of climate change from El'gygytgyn Crater lake, Northeastern Siberia, J. Paleolimnol., 37, 105–122, 2007.

Bassinot, F. C., Labeyrie, L. D., Vincent, E., Quidelleur, X., Shackleton, N. J., and Lancelot, Y.: The astronomical theory of climate and the age of the Brunhes–Matuyama magnetic reversal, Earth Planet. Sc. Lett, 126, 91–108, 1994.

Bely, V. F. and Belaya, B. V.: Late Stage of the OCVB Development (Upstream of the Enmyvaam River), NEISRI FEB RAS Press, Magadan, 1998.

Bely, V. F. and Raikevich, M. I.: The El'gygytgyn Lake Basin (Geological Structure, Morphostructure, Impactites, Problems of Investigation and Preservation of Nature), NEISRI FEB RAS Press, Magadan, 1994.

Bokhorst, M. P., Beets, C. J., Markovic, S. B., Gerasimenko, N. P., Matviishina, Z. N., and Frechen, M.: Pedo-chemical climate proxies in Late Pleistocene Serbiane–Ukrainian loess sequences, Quatern. Int., 198, 113–123, 2009.

Borkhodoev, V. Ya.: X-ray fluorescence determination of rubidium, strontium, yttrium, zirconium and niobium in rocks, J. Trace Microprobe T., 16, 341–352, 1998.

Borkhodoev, V. Ya.: Accuracy of the fundamental parameter method for x-ray fluorescence analysis of rocks, X-Ray Spectrom., 31, 209–218, 2002.

Boyle, J. F.: Inorganic geochemical methods in paleolimnology, in: Tracking Environmental Change Using Lake Sediments: Physical and Geochemical Methods, edited by: Last, W. M. and Smol, J. P., Springer, Berlin, 83–141, 2002.

Buggle, B., Glaser, B., Hambach, U., Gerasimenko, N., and Marković, S.: An evaluation of geochemical weathering indices in loesspaleosol studies, Quatern. Int., 240, 12–21, 2011.

Burov, B. V., Nourgaliev, D. K., and Yasonov, P. G.: Paleomagnetic Analysis, KGU Press, Kazan, 1986.

Cremer, H. and van de Vijver, B.: On Pliocaenicus costatus (*Bacillariophyceae*) in Lake El'gygytgyn, East Siberia, Eur. J. Phycol., 41, 169–178, 2006.

Darmody, R. G., Thorn, C. E., Harder, R. L., Schlyter, J. P. L., and Dixon, J. C.: Weathering implications of water chemistry in an arctic–alpine environment, northern Sweden, Geomorphology, 34, 89–100, 2000.

Title Page

Abstract | Introduction

Conclusions | References

Tables | Figures

Back | Close

Full Screen / Esc

Printer-friendly Version

Interactive Discussion

Das, B. K. and Haake, B.-G.: Geochemistry of Rewalsar Lake sediment, Lesser Himalaya, India; implications for source-area weathering, provenance and tectonic setting, Geosci. J., 7, 299–312, 2003.

Dasch, E. J.: Strontium isotopes in weathering profiles, deep-sea sediments and sedimentary rocks, Geochim. Cosmochim. Acta, 33, 1521–1552, 1969.

Davison, W.: Iron and manganese in lakes, Earth Sci. Rev., 34, 119–163, 1993.

de Jayawardena, U. S. and Izawa, E.: A new Chemical Index of Weathering for metamorphic silicate rocks in tropical regions: a study from Sri Lanka, Eng. Geol., 36, 303–310, 1994.

Duzgoren-Aydin, N. S., Aydin, A., and Malpas, J.: Re-assessment of chemical weathering indices: case study on pyroclastic rocks of Hong Kong, Eng. Geol., 63, 99–119, 2002.

Dypvik, H. and Harris, N. B.: Geochemical facies analysis of fine-grained siliciclastics using Th/U, Zr/Rb and (Zr + Rb)/Sr ratios, Chem. Geol., 181, 131–146, 2001.

Fagel, N., Alleman, L. Y., Granina, L., Hatert, F., Thamo-Bozso, E., Cloots, R., and Andre, L.: Vivianite formation and distribution in Lake Baikal sediments, Global Planet. Change, 46, 315–336, 2005.

Fedo, C. M., Nesbitt, H. W., and Young, G. M.: Unraveling the effects of potassium metasomatism in sedimentary rocks and paleosols, with implications for paleoweathering conditions and provenance, Geology, 23, 921–924, 1995.

Fralick, P. W. and Kronberg, B. I.: Geochemical discrimination of elastic sedimentary rock sources, Sediment. Geol., 113, 111–124, 1997.

Francke, A., Wennrich, V., Sauerbrey, M., Juschus, O., Melles, M., and Brigham-Grette, J.: Multivariate statistic and time series analyses of grain-size data in Quaternary sediments of Lake El'gygytgyn, NE Russia, Clim. Past Discuss., 9, 217–244, doi:10.5194/cpd-9-217-2013, 2013.

Gallet, S., Jahn, B., Lanoe, B. V. V., Dia, A., and Rossello, E.: Loess geochemistry and its implications for particle origin and composition of the upper continental crust, Earth Planet. Sci. Lett., 156, 157–172, 1998.

Goldberg, E. L., Phedorin, M. A., Grachev, M. A., Bobrov, V. A., Dolbnya, I. P., Khlystov, O. M., Levina, O. V., and Ziborova, G. A.: Geochemical signals of orbital forcing in the records of paleoclimates found in the sediments of Lake Baikal, Nucl. Instrum. Meth. A, 448, 384–393, 2000.

Goldberg, K. and Humayun, M.: The applicability of the Chemical Index of Alteration as a paleoclimatic indicator: an example from the Permian of the Paraná Basin, Brazil, Palaeogeogr. Palaeocl., 293, 175–183, 2010.

Hall, K., Thorn, C. E., Matsuoka, N., and Prick, A.: Weathering in cold regions: some thoughts
5   and perspectives, Prog. Phys. Geogr., 26, 577–603, 2002.

Harnois, L.: The CIW index: a new chemical index of weathering, Sediment. Geol., 55, 319–322, 1988.

Heiri, O., Lotter, A. F., and Lemcke, G.: Loss on ignition as a method for estimating organic and carbonate content in sediments: reproducibility and comparability of results, J. Paleolimnol.,
10   25, 101–110, 2001.

Howard, W.: Awarm future in the past, Nature, 388, 418–419. 1997.

Jouzel, J., Masson-Delmotte, V., Cattani, O., Dreyfus, G., Falourd, S., Hoffmann, G., Minster, B., Nouet, J., Barnola, J. M., Chappellaz, J., Fisher, H., Gallet, J. C., Johnsen, S. J., Leuenberger, M., Loulergue, L., Luethi, D., Oerter, H., Parrenin, F., Raisbeck, G., Raynaud, D.,
15   Schilt, A., Schwander, J., Selmo, E., Souchez, R., Spahni, R., Stauffer, B., Steffensen, J. P., Stenni, B., Stocker, T., Tison, J. L., Werner, A., and Wolff, E. W.: Orbital and millennial Antarctic climate variability over the past 800,000 years, Science, 317, 793–796, 2007.

Juyal, N., Pant, R. K., Basavaiah, N., Bhushan, R., Jain, M., Saini, N. K., Yadava, M. G., and Singhvi, A. K.: Reconstruction of Last Glacial to early Holocene monsoon variability from
20   relict lake sediments of the Higher Central Himalaya, Uttrakhand, India, J. Asian Earth Sci., 34, 437–449, 2009.

Kalugin, I., Daryin, A., Smolyaninova, L., Andreev, A., Diekmann, B., and Khlystov, O.: 800-yr-long records of annual air temperature and precipitation over southern Siberia inferred from Teletskoye Lake sediments, Quaternary Res., 67, 400–410, 2007.

25 Layer, P. W.: Argon-40/argon-39 age of the El'gygytgyn impact event, Chukotka, Russia, Meteorit. Planet. Sci., 35, 591–599, 2000.

Le Maitre, R. W., Streckeisen, A., Zanettin, B., Le Bas, M. J., Bonin, B., Bateman, P., Bellieni, G., Dudek, A., Efremova, S., Keller, J., Lamere, J., Sabine, P. A., Schmid, R., Sorensen, H., and Wool, A. R.: Igneous rocks, A Classification and Glossary of Terms, 2nd Edn., Recommen-
30   dation of the International Union of Geological Science Subcommission on the systematics of igneous rocks, Cambridge University Press, 254 pp., 2002.

Lisiecki, L. E. and Raymo, M. E.: A Pliocene-Pleistocene stack of 57 globally distributed benthic $\delta^{18}O$ records, Paleoceanography, 20, 1–17, 2005.

Title Page

Abstract | Introduction

Conclusions | References

Tables | Figures

◄ | ►

◄ | ►

Back | Close

Full Screen / Esc

Printer-friendly Version

Interactive Discussion

Loizeau, J.-L., Span, D., Coppee, V., and Dominik, J.: Evolution of the trophic state of Lake Annecy (eastern France) since the last glaciation as indicated by iron, manganese and phosphorus speciation, J. Paleolimnol., 25, 205–214, 2001.

Mackereth, F. J. H.: Some chemical observations on post-glacial lake sediments, Philos. T. Roy. Soc. B, 256, 165–213, 1966.

Maslov, A. V., Krupenin, M. T., and Gareev, E. Z.: Lithological, Lithochemical, and geochemical indicators of paleoclimate: evidence from Riphean of the Southern Urals, Lithol. Miner. Resour., 38, 427–446, 2003.

Melles, M., Brigham-Grette, J., Glushkova, O. Yu., Minyuk, P. S., Nowaczyk, N. R., and Hubberten, H.-W.: Sedimentary geochemistry of core PG1351 from Lake El'gygytgyn – a sensitive record of climate variability in the East Siberian Arctic during the past three glacial–interglacial cycles, J. Paleolimnol., 37, 89–104, 2007.

Melles, M., Brigham-Grette, J., Minyuk, P., Koeberl, C., Andreev, A., Cook, T., Fedorov, G., Gebhardt, C., Haltia-Hovi, E., Kukkonen, M., Nowaczyk, N., Schwamborn, G., Wennrich, V., and the El'gygytgyn Scientific Party: The Lake El'gygytgyn scientific drilling project – conquering Arctic challenges through continental drilling, Sci. Drill., 11, 29–40, 2011.

Melles, M., Brigham-Grette, J., Minyuk, P. S., Nowaczyk, N. R., Wennrich, V., DeConto, R. M., Anderson, P. M., Andreev, A. A., Coletti, A., Cook, T. L., Haltia-Hovi, E., Kukkonen, M., Lozhkin, A. V., Rosén, P., Tarasov, P., Vogel, H., and Wagner, B.: 2.8 million years of arctic climate change from Lake El'gygytgyn, NE Russia, Science, 337, 315–320, 2012.

Migdisov, A. A.: The titanium–aluminium relationship in sedimentary rocks, Geokhimiya, 2, 149–163, 1960.

Minyuk, P. S., Brigham-Grette, J., Melles, M., Borkhodoev, V. Ya., and Glushkova, O. Yu.: Inorganic geochemistry of El'gygytgyn Lake sediments (northeastern Russia) as an indicator of paleoclimatic change for the last 250 kyr, J. Paleolimnol., 37, 123–133, 2007.

Minyuk, P. S., Borkhodoev, V. Ya., and Goryachev, N. A.: Geochemical characteristics of sediments from Lake El'gygytgyn, Chukotka Peninsula, as indicators of climatic variations for the past 350 ka, Dokl. Earth Sci., 436, 94–97, 2011.

Minyuk, P. S., Subbotnikova, T. V., Brown, L. L., and Murdock, K. J.: Thermomagnetic properties of vivianite nodules, Lake El'gygytgyn, Northeast Russia, Clim. Past Discuss., 8, 4989–5027, doi:10.5194/cpd-8-4989-2012, 2012.

Nesbitt, H. W. and Young, G. M.: Early Proterozoic climates and plate motions inferred from major element chemistry of lutites, Nature, 299, 715–717, 1982.

Title Page

Abstract | Introduction

Conclusions | References

Tables | Figures

◀◀ | ▶▶

◀ | ▶

Back | Close

Full Screen / Esc

Printer-friendly Version

Interactive Discussion

Nesbitt, H. W. and Young, G. M.: Prediction of some weathering trends of plutonic and volcanic rocks based on thermodynamic and kinetic considerations, Geochim. Cosmochim. Acta, 48, 1523–1534, 1984.

Nolan, M. and Brigham-Grette, J.: Basic hydrology, limnology, and meteorology of modern Lake El'gygytgyn, Siberia, J. Paleolimnol., 37, 17–35, 2007.

Nowaczyk, N. R., Melles, M., and Minyuk, P.: A revised age model for core PG1351 from Lake El'gygytgyn, Chukotka, based on magnetic susceptibility variations tuned to Northern Hemisphere insolation variations, J. Paleolimnol., 37, 65–76, 2007.

Nowaczyk, N. R., Haltia-Hovi, E. M., Ulbricht, D., Wennrich, V., Kukkonen, M., Rosen, P., Vogel, H., Meyer-Jacob, C., Andreev, A., Lozhkin, A. V., and El'gygytgyn Scientific Party: Chronology of Lake El'gygytgyn sediments, Clim. Past., in preparation, 2013.

Ortega, B., Caballero, M., Lozano, S., Vilaclara, G., and Rodríguez, A.: Rock magnetic and geochemical proxies for iron mineral diagenesis in a tropical lake: Lago Verde, Los Tuxtlas, East-Central Mexico, Earth Planet. Sc. Lett., 250, 444–458, 2006.

Panizzo, V. N., Jones, V. J., Birks, H. J. B., Boyle, J. F., Brooks, S. J., and Leng, M. J.: A multi-proxy palaeolimnological investigation of Holocene environmental change, between c. 10 700 and 7200 years BP, at Holebudalen, southern Norway, Holocene, 18, 805–817, 2008.

Parker, A. G., Goudie, A. S., Stokes, S., White, K., Hodson, M. J., Manning, M., and Kennet, D.: A record of Holocene climate change from lake geochemical analyses in southeastern Arabia, Quaternary Res., 66, 465–476, 2006.

Pistolato, M., Quaia, T., Marinoni, L., Vitturi, L. M., Salvi, C., Salvi, G., Setti, M., and Brambati, A.: Grain size, mineralogy and geochemistry in Late Quaternary sediments from the Western Ross Sea outer slope as proxies for climate changes, in: Antarctica: Contributions to Global Earth Sciences, edited by: Fütterer, D. K., Damaske, D., Kleinschmidt, G., Miller, H., and Tessensohn, F., Springer-Verlag, Berlin, Heidelberg, New York, 423–432, 2006.

Price, J. R. and Velbel, M. A.: Chemical weathering indices applied to weathering profiles developed on heterogeneous felsic metamorphic parent rocks, Chem. Geol., 202, 397–416, 2003.

Prokopenko, A. A., Hinnov, L. A., Williams, D. F., and Kuzmin, M. I.: Orbital forcing of continental climate during the Pleistocene: a complete astronomically tuned climatic record from Lake Baikal, SE Siberia, Quaternary Sci. Rev., 25, 3431–3457, 2006.

Title Page

Abstract | Introduction

Conclusions | References

Tables | Figures

◄ | ►

◄ | ►

Back | Close

Full Screen / Esc

Printer-friendly Version

Interactive Discussion

Discussion Paper | Discussion Paper | Discussion Paper | Discussion Paper

Prokopenko, A. A., Bezrukova, E. V., Khursevich, G. K., Solotchina, E. P., Kuzmin, M. I., and Tarasov, P. E.: Climate in continental interior Asia during the longest interglacial of the past 500 000 years: the new MIS 11 records from Lake Baikal, SE Siberia, Clim. Past, 6, 31–48, doi:10.5194/cp-6-31-2010, 2010.

Reynolds, R. L., Rosenbaum, J. G., Rapp, J., Kerwin, M. W., Bradbury, J. P., Colman, S., and Adam, D.: Record of late Pleistocene glaciation and deglaciation in the southern Cascade Range, I. Petrological evidence from lacustrine sediment in Upper Klamath Lake, southern Oregon, J. Paleolimnol., 31, 217–233, 2004.

Roman-Ross, G., Depetris, P. J., Arribere, M. A., Guevara, S. R., and Cuello, G. J.: Geochemical variability since the Late Pleistocene in Lake Mascardi sediments, northern Patagonia, Argentina, J. S. Am. Earth Sci., 15, 657–667, 2002.

Roy, P. D., Caballero, M., Lozano, R., Ortega, B., Lozano, S., Pi, T., Israde, I., and Morton, O.: Geochemical record of Late Quaternary paleoclimate from lacustrine sediments of paleo-lake San Felipe, western Sonora Desert, Mexico, J. S. Am. Earth Sci., 29, 586–596, 2010.

Sapota, T., Aldahan, A., and Al-Aasm, I. S.: Sedimentary facies and climate control on formation of vivianite and siderite microconcretions in sediments of Lake Baikal, Siberia, J. Paleolimnol., 36, 245–257, 2006.

Schwamborn, G., Fedorov, G., Schirrmeister, L., Meyer, H., and Hubberten, H.-W.: Periglacial sediment variations controlled by lake level rise and Late Quaternary climate at El'gygytgyn Crater Lake, Arctic Siberia, Boreas, 37, 55–65, 2008.

Sharma, S., Joachimski, M., Sharma, M., Tobschall, H. J., Singh, I. B., Sharma, C., Chauhan, M. S., and Morgenroth, G.: Late glacial and Holocene environmental changes in Ganga plain, Northern India, Quaternary Sci. Rev., 23, 145–159, 2004.

Spahni, R., Chappellaz, J., Stocker, T. F., Loulergue, L., Hausammann, G., Kawamura, K., Flückiger, J., Schwander, J., Raynaud, D., Masson-Delmotte, V., and Jouzel, J.: Atmospheric methane and nitrous oxide of the Late Pleistocene from Antarctic ice cores, Science, 310, 1317–1321, 2005.

Taboada, T., Cortizas, A. M., García, C., and García-Rodeja, E.: Particle-size fractionation of titanium and zirconium during weathering and pedogenesis of granitic rocks in NW Spain, Geoderma, 131, 218–236, 2006.

Title Page

Abstract | Introduction

Conclusions | References

Tables | Figures

◀ | ▶

◀ | ▶

Back | Close

Full Screen / Esc

Printer-friendly Version

Interactive Discussion

Tanaka, K., Akagawa, F., Yamamoto, K., Tani, Y., Kawabe, I., Kawai T.: Rare earth element geochemistry of Lake Baikal sediment: its implication for geochemical response to climate change during the Last Glacial/Interglacial transition, Quaternary Sci. Rev., 26, 1362–1368, 2007.

Taylor, S. R. and McLennan, S. M.: The Continental Crust: its Composition and Evolution, Blackwell, London, 312 pp., 1985.

Vegas, J., Ruiz-Zapata, B., Ortiz, J. E., Galan, L., Torres, T., Garcıa-Cortes, A., Gil-Garcıa, M. J., Perez-Gonzalez, A., and Gallardo-Millan, J. L.: Identification of arid phases during the last 50 cal ka BP from the Fuentillejo maar-lacustrine record (Campo de Calatrava Volcanic Field, Spain), J. Quaternary Sci., 25, 1051–1062, 2010.

Wallmann, K., Aloisi, G., Haeckel, M., Tishchenko, P., Pavlova, G., Greinert, J., Kutterolf, S., and Eisenhauer, A.: Silicate weathering in anoxic marine sediments, Geochim. Cosmochim. Acta, 72, 3067–3090, 2008.

Weltje, G. J. and von Eynatten, H.: Quantitative provenance analysis of sediments: review and outlook, Sediment. Geol., 171, 1–11, 2004.

Wennrich, V., Francke, A., Dehnert, A., Juschus, O., Leipe, T., Vogt, C., Brigham-Grette, J., Minyuk, P. S., Melles, M., and El'gygytgyn Science Party: Modern sedimentation patterns in Lake El'gygytgyn, NE Russia, derived from surface sediment and inlet streams samples, Clim. Past Discuss., 8, 2007–2039, doi:10.5194/cpd-8-2007-2012, 2012.

White, A. F. and Blum, A. E.: Effects of climate on chemical weathering rates in watersheds, Geochim. Cosmochim. Acta, 59, 1729–1747, 1995.

Whitlock, C., Dean, W., Rosenbaum, J., Stevens, L., Fritz, S., Bracht, B., and Power, M.: A 2650-year-long record of environmental change from northern Yellowstone National Park based on a comparison of multiple proxy data, Quatern. Int., 188, 126–138, 2008.

Xiao, S., Liu, W., Li, A., Yang, S., and Lai, Z.: Pervasive autocorrelation of the chemical index of alteration in sedimentary profiles and its palaeoenvironmental implications, Sedimentology, 57, 670–676, 2010.

Yang, S., Ding, F., and Ding, Z.: Pleistocene chemical weathering history of Asian arid and semi-arid regions recorded in loess deposits of China and Tajikistan, Geochim. Cosmochim. Acta, 70, 1695–1709, 2006.

Yi, C., Liu, H., Rose, N. L., Yang, H., Ni, L., and Xie, P.: Sediment sources and the flood record from Wanghu Lake, in the middle reaches of the Yangtze River, J. Hydrol., 329, 568–576, 2006.

Young, G. M. and Nesbitt, H. W.: Processes controlling the distribution of Ti and Al in weathering profiles, siliciclastic sediments and sedimentary rocks, J. Sediment. Res., 68, 448–455, 1998.

Yudovich, Ya. E. and Ketris, M. P.: Geochemical Indicators of Lithogenesis, Geoprint, Syktyvkar, 742 pp., 2011.

Inorganic data from El'gygytgyn Lake sediments: stages 6–11

P. S. Minyuk et al.

Title Page

Abstract | Introduction

Conclusions | References

Tables | Figures

◄ | ►

◄ | ►

Back | Close

Full Screen / Esc

Printer-friendly Version

Interactive Discussion

Table 1. Correlation coefficients of Pearson (r) for major and trace elemental analyses from El'gygytgyn Lake sediments.

	SiO_2	Al_2O_3	TiO_2	Fe_2O_3	MnO	MgO	CaO	Na_2O	K_2O	P_2O_5	Rb	Zr	Sr	Ba	Ni	Cr
SiO_2	1.00															
Al_2O_3	**−0.89**	1.00														
TiO_2	−0.74	0.62	1.00													
Fe_2O_3	**−0.82**	0.49	0.69	1.00												
MnO	−0.26	0.01	0.22	0.51	1.00											
MgO	**−0.81**	0.77	**0.83**	0.65	0.08	1.00										
CaO	0.12	−0.04	−0.34	−0.38	−0.29	−0.29	1.00									
Na_2O	−0.04	0.02	0.10	−0.17	−0.12	−0.14	0.55	1.00								
K_2O	−0.47	0.64	−0.06	0.01	−0.31	0.22	0.49	0.31	1.00							
P_2O_5	−0.21	−0.16	0.03	0.56	0.55	−0.01	−0.25	−0.22	−0.29	1.00						
Rb	−0.66	**0.82**	0.19	0.22	−0.19	0.47	0.18	0.02	**0.89**	−0.22	1.00					
Zr	−0.63	0.55	**0.82**	0.48	0.13	0.55	0.01	0.53	0.22	−0.09	0.25	1.00				
Sr	0.19	−0.07	−0.38	−0.49	−0.34	−0.42	**0.83**	0.71	0.56	−0.31	0.23	0.08	1.00			
Ba	−0.47	0.55	0.13	0.07	−0.20	0.21	0.56	0.49	**0.86**	−0.22	0.69	0.38	0.62	1.00		
Ni	−0.12	0.07	0.21	0.14	0.09	0.12	−0.02	0.06	−0.04	0.01	−0.04	0.22	−0.05	0.01	1.00	
Cr	−0.38	0.25	0.60	0.47	0.21	0.50	−0.32	−0.09	−0.20	0.12	−0.04	0.42	−0.41	−0.11	**0.78**	1.00

Table 2. Correlation coefficients of Pearson (r) for selective elemental ratios and indices from El'gygytgyn Lake sediments.

	CIA	CIA$_{mol}$	CIW	PIA	CPA	1[*]	STI	Rb/Sr	Ba/Sr	LOI	MS	J_p
CIA	1.00											
CIA$_{mol}$	0.99	1.00										
CIW	0.97	0.97	1.00									
PIA	0.99	0.99	0.99	1.00								
CPA	0.92	0.92	0.97	0.96	1.00							
1[*]	−0.74	−0.72	−0.63	−0.68	−0.52	1.00						
STI	−0.73	−0.73	−0.69	−0.71	−0.56	0.78	1.00					
Rb/Sr	0.86	0.88	0.90	0.89	0.86	−0.54	−0.70	1.00				
Ba/Sr	0.73	0.76	0.75	0.74	0.67	−0.61	−0.76	0.85	1.00			
LOI	0.35	0.37	0.38	0.37	0.50	0.16	0.22	0.31	0.12	1.00		
MS	−0.66	−0.64	−0.57	−0.61	−0.57	0.52	0.36	−0.44	−0.35	−0.43	1.00	
J_p	0.73	0.73	0.67	0.70	0.65	−0.57	0.55	0.59	0.51	0.37	−0.88	1.00

1[*] – $(CaO + Na_2O + MgO)/TiO_2$
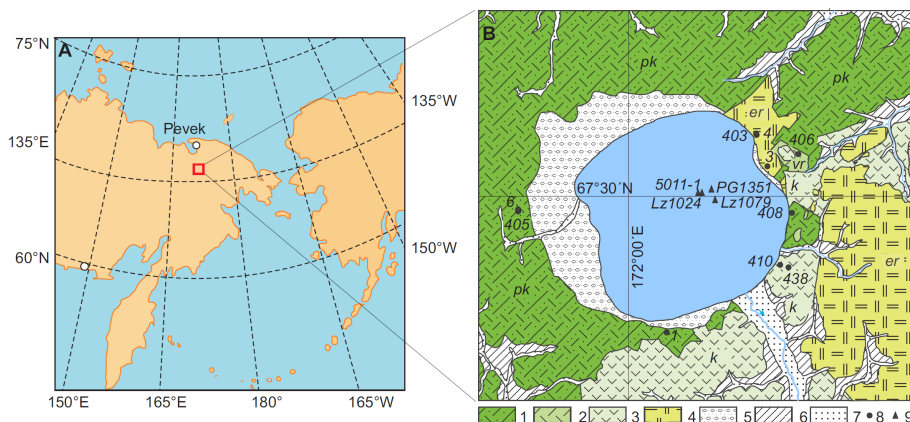
Fig. 1. Location **(A)** and geological map **(B)** of El'gygytgyn area adapted from Bely and Raikevich (1994); Bely and Belaya (1998). Formation: 1 – Pykarvaam (pk); 2 – Voronian (vr); 3 – Koekvun' (*k*); 4 – Ergyvaam (er); 5 – deluvian; 6 – terrace deposits; 7 – flood plain deposits; 8 – geochemical sites; 9 – cores.

Title Page

Abstract | Introduction

Conclusions | References

Tables | Figures

◀◀ | ▶▶

◀ | ▶

Back | Close

Full Screen / Esc

Printer-friendly Version

Interactive Discussion
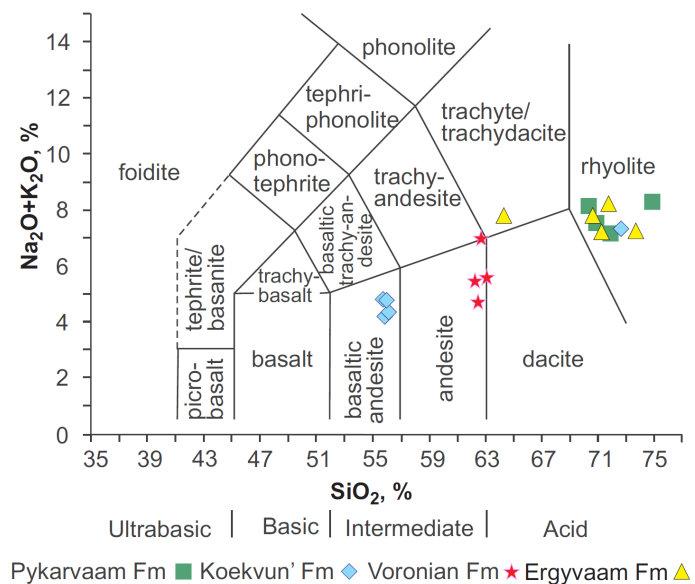
Fig. 2. Total alkali-silica diagram (Le Maitre et al., 2002) for volcanic rocks of El'gygytgyn area. Geochemical data from Bely and Belaya (1998).
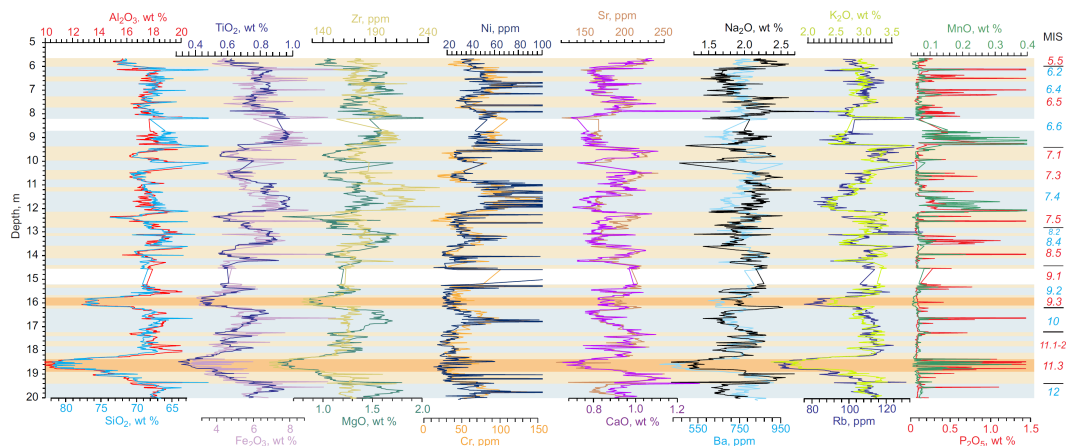
Fig. 3. Distribution of selected elements along the depth profile. Yellow bars are interglacials, orange bars are warmest substages, and blue bars are glacials. Marine isotopic stages (MIS) are showed according Bassinot et al. (1994). Note that SiO_2 is plotted on reverse scale.
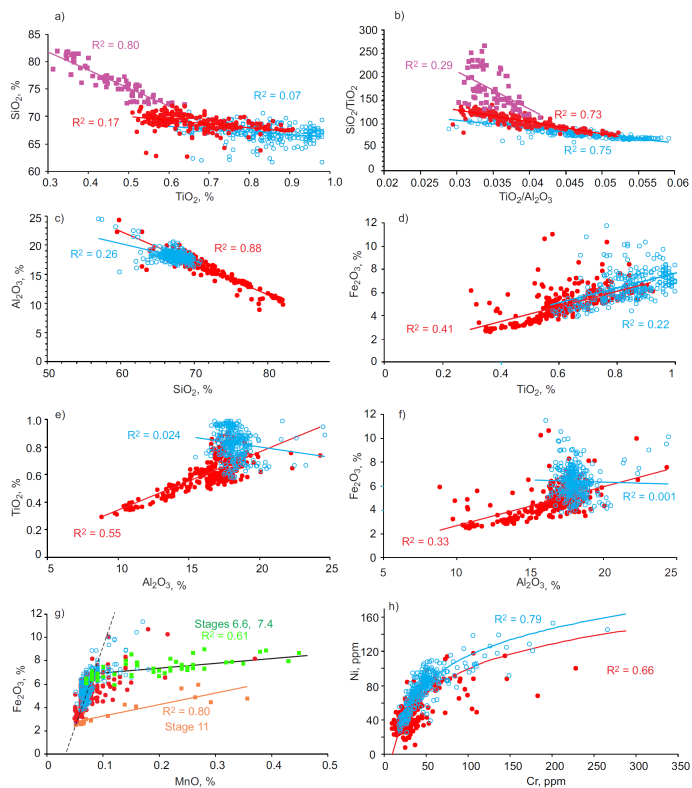
Fig. 4. Scatterplots showing the relationship between selected elements: **(a)** SiO_2 versus TiO_2, **(b)** SiO_2/TiO_2 versus TiO_2/Al_2O_3, **(c)** Al_2O_3 versus SiO_2, **(d)** Fe_2O_3 versus TiO_2, **(e)** TiO_2 versus Al_2O_3, **(f)** Fe_2O_3 versus Al_2O_3, **(g)** Fe_2O_3 versus MnO, **(h)** Ni versus Cr. Red (blue) symbols are interglacials (glacials), violet symbols are sediment with content of SiO_2 more then 71 %, orange symbols are stage 11, green symbols are stage 6.6 and 7.4.
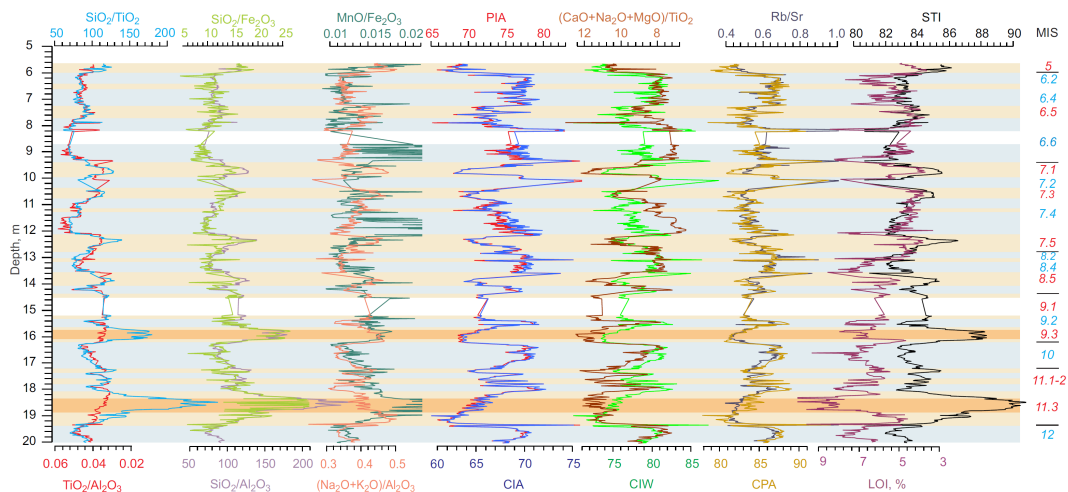
Fig. 5. Distribution of selected geochemical indices and ratios along the depth profile. Yellow bars are interglacials, orange bars are warmest substages, and blue bars are glacials. Marine isotopic stages (MIS) are showed according Bassinot et al. (1994). Note that LOI and $(CaO + Na_2O + K_2O)/TiO_2$ and TiO_2/Al_2O_3 are plotted on reverse scale.
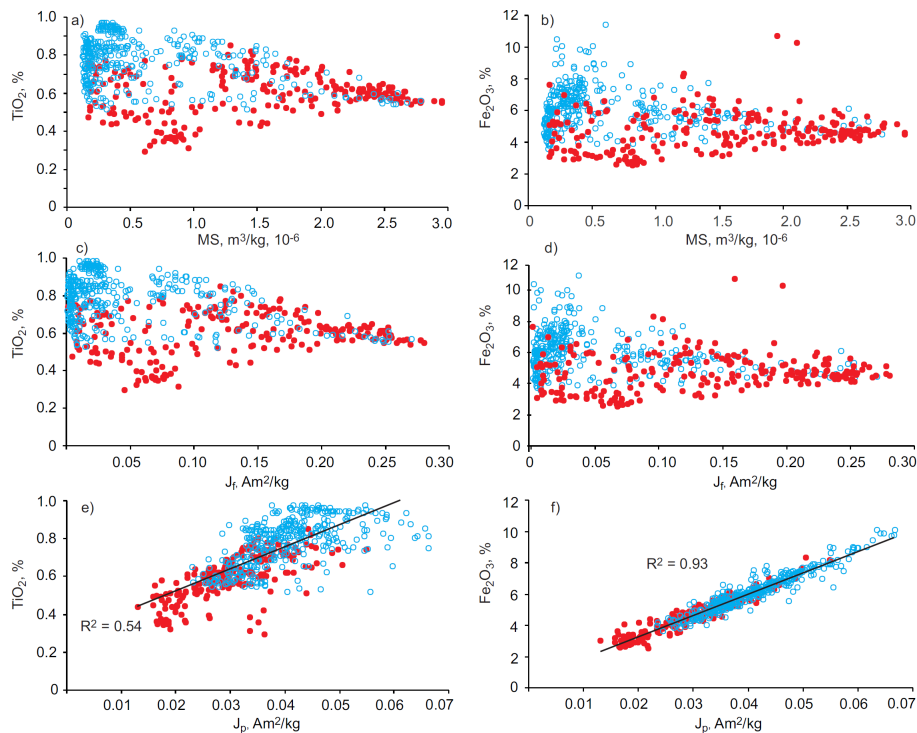
Fig. 6. Diagrams showing variations in TiO_2 and Fe_2O_3 vs. magnetic susceptibility, ferromagnetic and paramagnetic components of induced magnetization. Red (blue) symbols are interglacials (glacials).
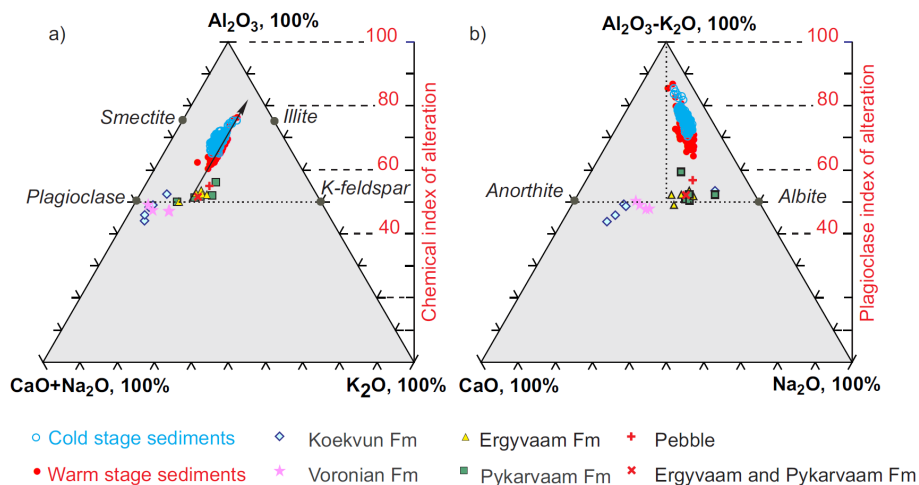
Fig. 7. Ternary diagrams showing of weathering trends of volcanic rocks and sediments: **(a)** (CaO + Na$_2$O)–Al$_2$O$_3$–K$_2$O diagram (Nesbitt and Young, 1984); **(b)** CaO–(Al$_2$O$_3$–K$_2$O)–Na$_2$O diagram (Fedo et al., 1995). Arrow indicates weathering trends.
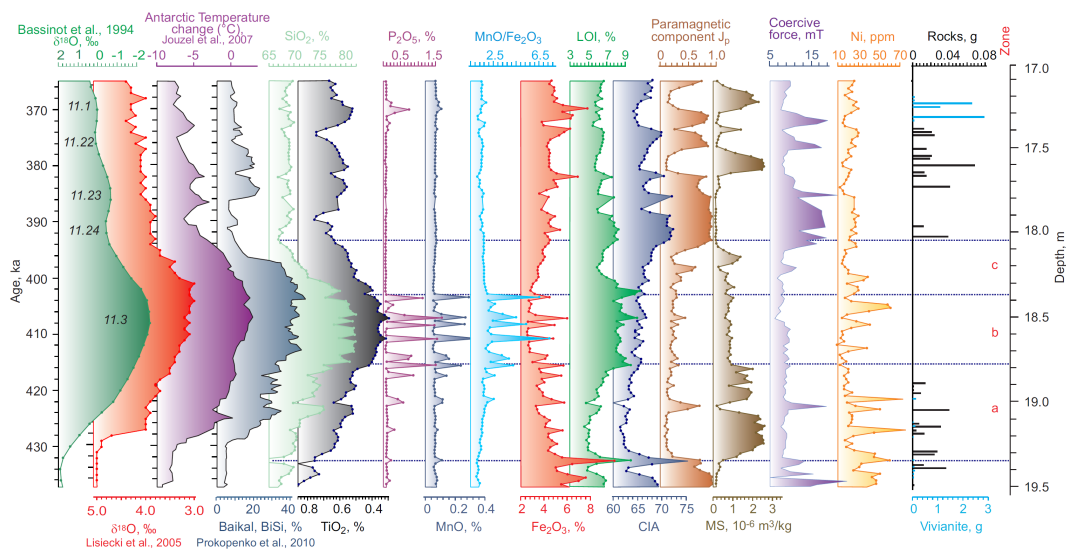
Fig. 8. Geochemical structure of MIS 11. Note that TiO$_2$ is plotted on reverse scale.
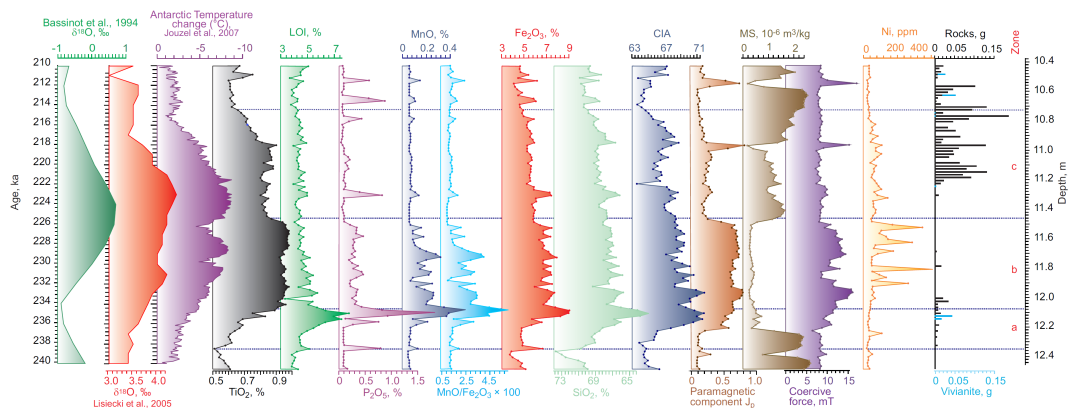
Fig. 9. Geochemical structure of MIS 7.4. Note that SiO$_2$ is plotted on reverse scale.

Inorganic data from El'gygytgyn Lake sediments: stages 6–11

P. S. Minyuk et al.